Published in final edited form as:

Cell Mol Life Sci. 2016 April ; 73(7): 1515–1528. doi:10.1007/s00018-015-2082-0.

Unconventional EGF-induced ERK1/2-mediated Kv1.3 endocytosis

Ramón Martínez-Mármol[1,2], **Núria Comes**[1], **Katarzyna Styrczewska**[1], **Mireia Pérez-Verdaguer**[1], **Rubén Vicente**[3], **Lluís Pujadas**[2], **Eduardo Soriano**[2,4,5], **Alexander Sorkin**[6], and **Antonio Felipe**[1,7]

Antonio Felipe: afelipe@ub.edu

[1]Molecular Physiology Laboratory, Departament de Bioquímica i Biologia Molecular, Institut de Biomedicina (IBUB), Barcelona, Spain

[2]Departament de Biologia Celular, Universitat de Barcelona, Barcelona, Spain

[3]Laboratory of Molecular Physiology and Channelopathies, Departament de Ciències Experimentals i de la Salut, Universitat Pompeu Fabra, Barcelona, Spain

[4]Centro de Investigación Biomédica en Red sobre Enfermedades Neurodegenerativas (CIBERNED), ISCIII, Madrid, Spain

[5]Vall d'Hebron Institute of Research (VHIR) and Institució Catalana de Recerca i Estudis Avançats (ICREA), Barcelona, Spain

[6]Department of Cell Biology, University of Pittsburgh School of Medicine, Pittsburgh, PA, USA

[7]Departament de Bioquímica i Biologia Molecular, Universitat de Barcelona, Avda. Diagonal 643, 08028 Barcelona, Spain

Abstract

The potassium channel Kv1.3 plays roles in immunity, neuronal development and sensory discrimination. Regulation of Kv1.3 by kinase signaling has been studied. In this context, EGF binds to specific receptors (EGFR) and triggers tyrosine kinase-dependent signaling, which down-regulates Kv1.3 currents. We show that Kv1.3 undergoes EGF-dependent endocytosis. This EGF-mediated mechanism is relevant because is involved in adult neural stem cell fate determination. We demonstrated that changes in Kv1.3 subcellular distribution upon EGFR activation were due to Kv1.3 clathrin-dependent endocytosis, which targets the Kv1.3 channels to the lysosomal degradative pathway. Interestingly, our results further revealed that relevant tyrosines and other interacting motifs, such as PDZ and SH3 domains, were not involved in the EGF-dependent Kv1.3 internalization. However, a new, and yet undescribed mechanism, of ERK1/2-mediated threonine phosphorylation is crucial for the EGF-mediated Kv1.3 endocytosis. Our results demonstrate that EGF triggers the down-regulation of Kv1.3 activity and its expression at the cell surface, which is important for the development and migration of adult neural progenitors.

Correspondence to: Antonio Felipe, afelipe@ub.edu.

Electronic supplementary material The online version of this article (doi:10.1007/s00018-015-2082-0) contains supplementary material, which is available to authorized users.

Keywords

Olfactory bulb; Sensory neurons; Map kinases; Tyrosine kinases; Endocytosis; Voltage-dependent potassium channels

Introduction

The dentate gyrus of the hippocampal formation and the subventricular zone (SVZ) of the forebrain are considered the main loci of adult neurogenesis [1]. Cellular proliferation in the SVZ of healthy adult rodents supplies progenitor cells to the olfactory bulb (OB) via the rostral migratory stream (RMS), where they contribute to the replacement of granular and periglomerular neurons [2]. However, in response to injury, SVZ cells proliferate, migrate and differentiate into specific neuronal populations, astrocytes and oligodendrocytes [3]. Epidermal growth factor (EGF) is a mitogen involved in regulating neural stem cell proliferation and differentiation. Infusion of EGF into the lateral ventricle not only modulates proliferation but also results in SVZ cells altering their migration from their normal route and into adjacent areas of the brain [4]. Therefore, the role of EGF-mediated effects in the neural precursors of the SVZ is essential for their final differentiation and function. The EGF receptor (EGFR) is expressed at high levels in the nervous system and exhibits regionalized patterns of distribution during the initial phases of development and in the adult [5]. EGFR activation initiates a downstream serine/threonine and tyrosine phosphorylation-based signaling cascade that modulates the activity of a wide range of heterogeneous proteins, including ion channels [6].

Voltage-gated potassium channels (Kv) have a crucial role in excitable cells by determining the resting membrane potential and controlling action potentials [7]. The Kv1.3 channel controls action potential firing of hippocampal and OB neurons, accounting for up to 60–80 % of the outward K^+ currents [8]. This channel is also predominantly expressed in the mitral and granule nerve cell layers and in postganglionic sympathetic neurons, as well as in brain progenitor cells [9]. Interestingly, the gene-targeted deletion of the Kv1.3 channel ($Kv1.3^{-/-}$) generates mice with altered interneuron populations of the cerebral cortex, and a highly developed olfactory function due to an increase of olfactory coding units in the OB [10]. The Kv1.3 channel is also critical in leukocytes participating in physiological responses such as cell proliferation, activation or migration [11, 12]. Kv1.3 can be phosphorylated by receptor (EGFR, TrkB and insulin receptor) and non-receptor tyrosine kinases (src and leukocyte-specific protein tyrosine kinase (Lck)), modulating channel kinetics and current amplitude [8, 10, 13–18]. In addition to kinase signaling, evidence has shown that the prevalence of Kv1.3 channels at the membrane surface have enormous consequences for cell physiology [19–22]; thus, ion channel-induced endocytosis mechanisms have attracted considerable attention. Ion channels, such as ENaC, K_{ATP} and CFTR, are internalized via clathrin-mediated endocytosis (CME) [23–25]. Furthermore, endocytosis is a mechanism for tyrosine kinase-dependent suppression of the neuronal Kv1.3-related channel Kv1.2 [26]. However, Kv1.3 tyrosine-phosphorylation is not accompanied by channel endocytosis [27]. Thus, it remains unclear whether Kv1.3 suppression may involve endocytosis as a relevant turnover mechanism.

Here, we report that suppression of Kv1.3 activity upon incubation with EGF was partially due to specific channel internalization. EGFR activation triggers channel endocytosis through a clathrin-dependent mechanism, which is independent of putative EGF-mediated Kv1.3 tyrosine phosphorylation. Interestingly, EGF mediates channel endocytosis via a novel ERK1/2-dependent threonine phosphorylation mechanism. This EGF-dependent Kv1.3 down regulation is crucial for the understanding of the proliferative and migratory behavior of specific neuronal populations of the forebrain.

Materials and methods

Animals, primary culture of SVZ explants and neuronal stem precursors cells (NSPCs) grown as neurospheres and immunohistochemistry

All of the experiments and surgical protocols were performed in accordance with the guidelines approved by the ethical committee of the Universitat de Barcelona following the European Community Council Directive 86/609 EEC. P5 newborn mice were anesthetized with 4 % halothane and were transcardially perfused with 4 % paraformaldehyde dissolved in phosphate buffer 0.12 M (pH 7.2–7.4). After perfusion, the brains were removed from the skull and postfixed in the same solution for an additional 12 h, cryoprotected in 30 % sucrose, and coronally sectioned on a freezing microtome (30 μm thick). Free-floating sections were permeabilized with PBS containing 0.5 % Triton X-100 and blocked with 10 % normal goat serum. The brain sections were incubated with anti-Kv1.3 (1:500 Alomone) and anti-EGFR (1:500, SantaCruz) antibodies and visualized using secondary fluorescent antibodies (Alexa 488 and 568, 1:1000, Invitrogen). Immunoreagents were diluted in PBS containing 0.5 % Triton X-100, 0.2 % gelatin, and 5 % pre-immune serum.

Experiments studying SVZ explant migration have been previously documented [28]. Briefly, SVZ explants were obtained as previously described [29]. P1–P3 newborn mice were anesthetized by hypothermia and then euthanized by rapid decapitation. Brains were removed and placed in ice-cold dissection medium (0.6 % glucose in PBS). After vibratome sectioning, the SVZ from the lateral wall of the anterior horn of the lateral ventricle was dissected out from the appropriate section and cut into pieces of 100–300 mm in diameter. The explants were mixed with Matrigel (BD Bioscience) and cultured in four-well dishes. After polymerization for 10 min, the gel was overlaid with 0.5 ml of growth medium (Neurobasal medium containing 0.5 mM L-glutamine and penicillin–streptomycin antibiotics and 2 % B-27). Cultures were maintained in a humidified, 5 % CO_2, 37 °C incubator for 7 days. EGF (10 ng/ml) and 30 nM Margatoxin, an inhibitor of Kv1.3, were added to the medium. After 7 days in vitro, tissue cultures were fixed with paraformaldehyde (4 % in 0.1 M PBS) and type-B astrocytes were visualized immunostaining against GFAP (1:1000, Dako), followed by Alexa 488 secondary antibodies (1:500, Invitrogen). Images were acquired using an Olympus Scan^R wide field microscope (10× objective lenses) and automated 5 × 6 mosaic acquisition was performed using Scan^R software. Mosaics were reconstructed using the FIJI Stitching plugin and the signal intensity was analyzed using the FIJI Radial Profile Plot plugin. Plotted values represent the integrated intensity of concentric circles emerging from the center of the explants. Neuronal stem precursor cells (NSPC) grown as neurospheres were obtained from the SVZ of P1–P3

newborn mice as previously described [30] in growth medium supplemented with 2 % B27 and 20 ng/ml EGF and bFGF (R&D System). Twenty-four hours after the 3rd passage, neurospheres were transferred to poly-D-lysine-coated dishes, and electrophysiology of the adherent cells was performed 16 h later. For immunostaining, neurospheres were embedded in rat tail Collagen I (BD Biosciences), fixed with paraformaldehyde (4 % in 0.1 M PBS) and processed for immunodetection. Primary cultures of SVZ-derived cells were obtained by culturing SVZ-derived cells for 8–12 h in growth medium supplemented with 2 % B27. Finally, neurospheres and SVZ cells were immunostained against Kv1.3 (rabbit, Alomone 1:500; mouse, NeuroMab 1:250), EGFR (rabbit, SantaCruz 1:250) and Nestin (mouse, R&D Systems 1:500). Images were obtained using a Leica SP2 Spectral Confocal microscope.

Expression plasmids and site-directed mutagenesis

The rat Kv1.3 in pRcCMV construct was provided by T.C. Holmes (New York University, NY). The channel was subcloned into pEYFP-C1 (Clontech). The rKv1.3 construct that was externally tagged with HA between S3 and S4 was obtained from D.B. Arnold (University of Southern California, CA). All Kv1.3 mutants were generated in the pEYFP-Kv1.3 channel. Single and multiple Kv1.3 mutants were generated using the QuikChange and QuikChange multi-site-directed mutagenesis kits (Stratagene). All mutations were verified using automated DNA sequencing. The pEGFR-GFP construct has been extensively characterized by Sorkin's laboratory [31].

Cell culture, transfections and EGF incubations

HEK-293 and HeLa cells were grown in DMEM containing 10 % FBS and 100 U/ml penicillin/streptomycin. For the confocal analyses, cells cultured in the same medium were plated on poly-lysine-coated coverslips. Transfection was performed using Metafectene™ Pro (Biontex) when cells reached nearly 80 % confluence. For transient transfection, the cells were washed in PBS (without K^+), fixed with 4 % paraformaldehyde in PBS for 10 min and mounted with Aqua Poly/Mount from Polysciences, Inc. at 24 h after transfection. Because HeLa cells express a high number of endogenous EGFR [32], a HeLa cell line with stable Kv1.3-YFP expression was generated. Twenty-four hours after transfection, cells were selected in the presence of 500 μg/ml G418. Geneticin-resistant clones were isolated and maintained in the presence 250 μg/ml G418. In some experiments, transiently transfected HEK-293 and HeLa cells were pre-incubated with 50 μM erbstatin or 10 μM U0126, respectively, for 1 h prior to incubation with EGF. Cells cultured for 24 h in the absence of serum were further incubated for 1 h at 4 °C in the presence of 10 ng/ml or 4 ng/ml EGF-rhodamine, for HEK and HeLa cells, respectively, and transferred to 37 °C for the desired times before analysis.

Protein extraction, co-immunoprecipitation, biotinylation of cell surface proteins and western blot analysis

Cells were washed twice in cold PBS. Next, they were lysed on ice with NHG solution (1 % Triton X-100, 10 % glycerol, 50 mM HEPES pH 7.2, 150 mM NaCl) supplemented with 1 μg/ml aprotinin, 1 μg/ml leupeptin, 1 μg/ml pepstatin and 1 mM phenylmethylsulfonyl fluoride to inhibit proteases. The homogenates were centrifuged at 16,000×*g* for 15 min, and the protein content was measured using the Bio-Rad Protein Assay (Bio-Rad).

The samples were pre-cleared with 30 µl of protein G-Sepharose beads for 2 h at 4 °C with gentle mixing as part of the co-immunoprecipitation procedure. The beads were then removed by centrifugation at 1000×*g* for 30 s at 4 °C. The sample was then incubated overnight with the desired antibody (4 ng/µg protein) at 4 °C with gentle agitation. Thirty microliters of protein G-Sepharose were added to each sample, and the samples were incubated for 4 h at 4 °C. The beads were removed by centrifugation at 1000×*g* for 30 s at 4 °C, washed four times in NHG, and resuspended in 80 µl of SDS sample buffer.

Cell surface biotinylation was carried out with the Pierce® Cell Surface Protein Isolation Kit (Pierce) following manufacturer's instructions. Cell surface proteins were labeled with sulfosuccinimidyl-2-(biotinamido)ethyl-1,3-dithiopropionate (Sulfo-NHS-SS-biotin; Pierce) as previously described. Briefly, cells were treated with lysis buffer and clear supernatant was reacted with immobilized NeutrAvidin gel slurry in columns (Pierce) to isolate surface proteins. Surface proteins were resolved on a SDS-PAGE gel and analyzed by western blot analysis against Kv1.3.

Protein samples (50 µg) and immunoprecipitates were then boiled in Laemmli SDS loading buffer and separated by 10 % SDS-PAGE. Next, samples were transferred to nitrocellulose membranes (Immobilon-P, Millipore) and blocked in 5 % dry milk-supplemented with 0.05 % Tween 20 in PBS before the immunoreaction. Filters were then immunoblotted with antibodies against HA (1/200, Sigma), GFP (1/1000, Roche), T-ERK1/2, P-ERK1/2 and P-Thr (1/1000, Cell signaling), P-Tyr (1/2000, Sigma), Clathrin heavy chain (1/500, BD Bioscience), Dynamin II (1/1000, ABR) and β-actin (1/50,000, Sigma).

Confocal microscopy and subcellular compartment identification

Staining with specific markers to label subcellular compartments was performed on permeabilized cells. Cells fixed with 4 % paraformaldehyde in PBS for 10 min were further permeabilized using 0.1 % Triton for 10 min. After a 60 min incubation with a blocking solution (10 % goat serum/5 % non-fat dry milk/PBS), the cells were treated with anti-clathrin heavy chain (1/100, BD Bioscience) or anti-EEA1 (1/1000, BD Bioscience) in 10 % goat serum/0.05 % Triton and again incubated for 1 h. Next, the cells were further incubated for 45 min with an Alexa Fluor antibody (1/500, Molecular Probes) in PBS. All experiments were performed at room temperature. In some experiments, the cells were washed with PBS and stained with Lyso Tracker® red (1/1000, Molecular Probes) for 30 min at 4 °C. The amount of internalized Kv1.3-YFP channel (arbitrary units) was calculated by using a pixel by pixel analysis, taking into account the relative amount of intracellular signal versus the total signal in control experiments versus different conditions. Cells were examined with a 63× oil immersion objective on a Leica TCS SL laser scanning confocal microscope. All offline image analyses were performed using a Leica confocal microscope, Image J software and Sigma Plot.

siRNA transfections

Synthetic siRNAs for CHC and Dynamin II were purchased from Thermo Fisher Scientific. Duplexes were resuspended in 1 × siRNA universal buffer (Thermo Fisher Scientific) to 20 µM. HeLa cells expressing the stable Kv1.3-YFP channel were grown in six-well plates to

50 % confluence. Cells were transfected with siRNA duplexes at a final concentration of 120 nM in 5 μl DharmaFECT1 reagent (Thermo Fisher Scientific). After 36 h, a second transfection was performed, and the cells were replated in 12-well plates on the next day for internalization experiments. To assess the efficiency of knockdown, total cell lysates were resolved on 7.5 or 10 % SDS-PAGE depending on the protein of interest and probed by western blotting. Mock- or siRNA-transfected cells were processed for immunofluorescence as described above.

Antibody feeding endocytosis assay

Cells grown on glass coverslips or 96-well plates were incubated with 1–2 μg/ml of anti-HA11 (1/1000, Covance) in DMEM for 30–60 min at 18–20 °C, washed twice and incubated at 37 °C in the presence or in the absence of 4 ng/ml EGF-rhodamine for 30 min. The cells were then washed with ice-cold Ca^{2+}, Mg^{2+}-free PBS (CMF-PBS) and fixed with freshly prepared 4 % paraformaldehyde for 8 min at room temperature. The cells were stained with anti-mouse secondary antibody conjugated with Cy5 (5 μg/ml, saturating concentration) in CMF-PBS containing 0.5 % BSA at room temperature for 60 min to label the HA11 antibody on the surface. After washing, the cells were permeabilized in CMF-PBS containing 0.1 % Triton X-100 for 10 min at room temperature, and then incubated with the same secondary conjugated with Cy3 (1 μg/ml, non-saturating concentrations) for 60 min to stain internalized HA11. Both primary and secondary antibody solutions were precleared by centrifugation at 100,000×g for 20 min. After staining, cells were washed and the coverslips were mounted in Mowiol (Calbiochem).

Internalization of EGF-rhodamine

To highlight the intracellular EGF-enriched vesicles which colocalized with endocytosed Kv1.3 in HeLa cells, an acid wash protocol was performed as previously described [33]. As the acid wash removes completely the EGF-rhodamine attached to cell surface, only intracellular EGF-rhodamine remained in acid wash-treated cells. Briefly, cells cultured in 12-well dishes were incubated with EGF-rhodamine (4 ng/ml) in binding medium (DMEM, 20 mM HEPES, 0.1 % BSA) at 37 °C for 30 min. After incubation, the remaining EGF was removed from cell surface by a 5 min incubation with a prechilled mild acid wash (0.2 M sodium acetate, 0.5 M NaCl, pH 4.5) or binding medium wash (no acid). Samples were processed for fluorescence microscopy as above.

Electrophysiology

Whole-cell currents were recorded using the patch-clamp technique in the whole-cell configuration with a HEKA EPC10 USB amplifier (HEKA Elektronik). PatchMaster software (HEKA) was used for data acquisition. We applied a stimulation frequency of 50 kHz and a filter at 10 kHz. The capacitance and series resistance compensation were optimized. In most experiments, we obtained an 80 % compensation of the effective access resistance. Micropipettes were prepared from borosilicate glass capillaries (Harvard Apparatus) using a P-97 puller (Sutter Instrument) and fire polished. The pipettes had a resistance of 2–4 MΩ. For the stably transfected HeLa cells, pipettes were filled with a solution containing (in mM): 120 KCl, 1 $CaCl_2$, 2 $MgCl_2$, 10 HEPES, 10 EGTA, and 20 D-glucose (pH 7.3 and 280 mOsm/l). The extracellular solution contained (in mM): 120 NaCl,

5.4 KCl, 2 $CaCl_2$, 1 $MgCl_2$, 10 HEPES and 25 D-glucose (pH 7.4 and 310 mOsm/l). To record the currents of SVZ neurons we used an intracellular solution containing (in mM): 145 KF, 1 $MgCl_2$, 10 HEPES, 10 EGTA (pH 7.2). The extracellular solution for the native currents contained (in mM): 160 NaCl, 4.5 KCl, 2 $CaCl_2$, 1 $MgCl_2$, and 5 HEPES (pH 7.4). Cells were clamped at a holding potential of −60 mV. To evoke voltage-gated currents, all cells were stimulated with a 250-ms square pulse from −60 to +70 mV. The peak amplitude (pA) was normalized using the capacitance values (pF). Data analysis was performed using FitMaster (HEKA) and Sigma Plot 10.0 software (Systat Software). All recordings were performed at room temperature (21–23 °C).

Results

EGFR and Kv1.3 are expressed in SVZ-derived neurons and cooperate in their differentiation

The SVZ of the forebrain supplies progenitor cells to OB where EGF is a major growth factor [5]. Furthermore, the genetic depletion of Kv1.3 produces a super-smeller phenotype, which would suggest that EGF-dependent down-regulation of Kv1.3 would be an important determinant for olfactory capacities [10, 13]. Therefore, we first confirmed Kv1.3 expression in the OB (Fig. 1a). In addition, Kv1.3 partially colocalized with EGFR in the SVZ, which is a main locus of adult neurogenesis, (Fig. 1b). To gain further insights, we cultured isolated NSPCs and confirmed the co-expression of EGFR and Kv1.3 (Fig. 1c, d) in Nestin-positive SVZ-derived progenitor cells. Nestin was used to identify multipotent neuronal stem cells. Next, we generated SVZ-derived neurospheres, which were subsequently allowed to differentiate. Neurosphere-derived neurons were heavily stained for Kv1.3 (Fig. 1e). In addition, K^+ currents elicited in neurospheres diminished upon EGF incubation (Fig. 1f). Surprinsingly, K^+ currents, in the absence but not in the presence of EGF, were efficiently blocked by 100 nM MgTx, suggesting that Kv1.3 plays a major role in neuronal stem cells (NSC). We next studied the relevance of Kv1.3 and EFG in SVZ explant migration and differentiation by GFAP staining (Fig. 1g). We found that both 10 ng/ml EGF (0.37 ± 0.04, p <0.001) and 100 nM MgTx (0.20 ± 0.02, p <0.01) notably increased neuronal migration and differentiation (vs control, 0.13 ± 0.02; Student's t test at 500 μm) (Fig. 1h, i). Furthermore, incubation with both EGF and MgTx further enhanced the areas containing SVZ-derived migrating cells, suggesting synergistic cooperation of both pathways (0.50 ± 0.06, p <0.001). Together, our results demonstrate that Kv1.3 and EGFR are co-expressed in the SVZ in vivo as well as in SVZ-derived NSPCs and that the suppression of Kv1.3 channel activity leads to a marked increase in both neurogenesis and migration in the SVZ.

EGF-mediated Kv1.3 endocytosis in HEK-293 cells

Although tyrosine kinase receptor activation triggers the endocytosis of channels and EGF efficiently inhibits Kv1.3 currents, their ability to induce Kv1.3 endocytosis remains controversial [13, 26]. Therefore, we incubated EGFR and Kv1.3 co-transfected HEK-293 cells with EGF (10 ng/ml). EGF activated the EGFR as demonstrated by the detection of tyrosine phosphorylated EGFR (Supplementary Fig. 1A). As expected, EGFR also underwent endocytosis in these cells (Supplementary Fig. 1B). Supplementary Fig. 1C and D demonstrated that Kv1.3 currents were diminished by EGF and that the blockade of the

tyrosine kinase-EGFR activity by Erbstatin abolished this effect. EGF reduced Kv1.3 activity via a tyrosine kinase-dependent mechanism without affecting the abundance of the Kv1.3 protein (Supplementary Fig. 1E).

Next, we monitored the time course of Kv1.3 distribution in the presence of EGF. Figure 2 demonstrated that EGF caused Kv1.3 endocytosis. In the absence of EGF, Kv1.3 and EGFR were primarily localized at the cell surface (Fig. 2a–c); EGF incubation triggered the co-internalization of Kv1.3 and the EGFR (Fig. 2d–o). After 2 min of EGF incubation, only a few vesicles containing Kv1.3/EGFR/EGF were observed (Fig. 2d–g). However, longer periods of time triggered a massive increase in the number of intracellular vesicles with Kv1.3, EGFR and EGF colocalization (Fig. 2h–o). Co-immunoprecipitation studies (Fig. 2p) demonstrated that although Kv1.3 and EGFR shared intracellular compartments, the proteins did not associate. Similar negative results were obtained by Fluorescence Resonance Energy Transfer (FRET) studies between EGFR-CFP and Kv1.3-YFP.

EGF-dependent Kv1.3 endocytosis via clathrin-coated pits targeted the channel to lysosomes

To further investigate EGF-mediated Kv1.3 endocytosis, we used the HeLa cell line. HeLa cells express a significant amount of endogenous EGFR; therefore, the EGF-dependent signal transduction pathway is well preserved [32]. In addition, we generated a Kv1.3 stable HeLa cell line. Because Kv1.3 turnover is very rapid, we first wanted to decipher whether Kv1.3-containing vesicles were indeed a consequence of EGF-dependent endocytosis. Some intracellular Kv1.3 staining was observed in the absence of EGF (Supplementary Fig. 2A–B). When cells were incubated with non-saturating EGF concentrations (4 ng/ml), endocytic vesicles containing Kv1.3 were detected (Supplementary Fig. 2C–Hf). A mild acid wash eliminates excess unbound EGF at the cell surface and facilitates the analysis of the intracellular distribution of EGF and Kv1.3 (Supplementary Fig. 2F–H). Thus, the acid-wash magnified the Kv1.3-YFP/EGF-rhodamine colocalization because a notable decrease in the background signal corresponding to non-internalized rhodamine fluorophore was observed (compare Supplementary Fig. 2E and H). An “antibody feeding” assay paradigm has proven to be critical for deciphering the PKC-dependent endocytosis of the dopamine transporter (DAT) [34]. In HeLa cells transfected with HA-Kv1.3, the channels stained with Cy5-labeled antibodies were distributed as numerous small clusters throughout the plasma membrane (Supplementary Fig. 2I, L). In the absence of EGF, some Cy3-labeled intracellular vesicles were observed, which may correspond to endosomes containing constitutively internalized channels (Supplementary Fig. 2J). However, upon EGF incubation, an increase of Kv1.3 containing Cy3-labeled vesicles was noted (Supplementary Fig. 2M). Our results indicated that the intracellular complexes of the channel were inaccessible to the Cy5-labeled secondary antibodies applied to non-permeabilized cells, thereby confirming that the internal Cy3-labeled channels were indeed triggered by EGF (Supplementary Fig. 2L–N).

EGF activation caused accumulation of Kv1.3 in vesicular endocytic structures moving from peripheral to perinuclear areas. This occurred concomitantly with a decrease in the plasma membrane fluorescence (Fig. 3a, g). To further characterize the EGF-dependent Kv1.3

endocytic mechanisms, markers of each intracellular compartment were used. Thus, after 10 min, Kv1.3 and EGF colocalized with CHC, a marker of clathrin-coated pits (CCP) (Fig. 3a–g). After 30 min of EGF incubation, Kv1.3 and EGF distributed within early endosomes, which were labelled with EEA1 (Fig. 3h–n). Similar results were obtained with other markers such as AP2 and Transferrin Receptor (TfnR). Finally, to examine whether Kv1.3 is targeted to the late endosomes and lysosomes due to EGFR activation, the localization of the channel was compared with that of the late endosome marker, Lyso Tracker® Red (Fig. 3o–u). Our results demonstrated that EGF triggered a down regulation of the Kv1.3 channel on the membrane surface via CCP that facilitated Kv1.3 turnover through lysosomal degradation.

To decipher the mechanisms involved in clathrin-mediated EGF-dependent Kv1.3 endocytosis, we incubated the HeLa cells with siRNAs against CHC and dynamin II (Fig. 4). Both clathrin and dynamin II are crucial for the CME of TfnR, EGFR and DAT [35, 36]. Both siRNAs effectively depleted CHC and dynamin II (Fig. 4a, b), although depletion was not complete (estimated more than 95 %) as shown in Fig. 4o (clathrin-positive staining encircled the cell). Under these conditions, HeLa cells stably expressing Kv1.3 and transfected with CHC siRNA were incubated without (Fig. 4j–l) or with (Fig. 4m–p) EGF for 30 min at 37 °C. No significant EGF-dependent internalization of Kv1.3 was observed in siRNA-depleted CHC cells (compare Fig. 4m, f). In addition, TfnR internalization is typically halted by Dynamin II depletion (Fig. 4r, v). Concomitantly, EGFR activation-induced Kv1.3 endocytosis was also abolished with a specific siRNA for dynamin II (Fig. 4q–w; compare Fig. 4t, f). Together, the efficient inhibition of Kv1.3 endocytosis in CHC- and dynamin II-depleted cells demonstrated that CCP-mediated endocytosis is the main pathway for EGFR-induced Kv1.3 internalization.

EGF-mediated Kv1.3 endocytosis via ERK1/2 threonine phosphorylation

EGF triggered CCP-mediated Kv1.3 endocytosis, targeting the channel to the lysosomes and thereby controlling Kv1.3 turnover. Therefore, we wanted to decipher the structural elements responsible for this event. We first confirmed that EGFR-tyrosine kinase activity was responsible for the Kv1.3 endocytosis. Thus, Erbstatin efficiently inhibited the EGF-dependent endocytosis of Kv1.3 (Supplementary Fig. 3A–E). The role of several important tyrosines in the Kv1.3 channel activity has been analyzed, and raised controversial results because the evidence suggests that those residues were not related to the channel internalization [27]. To decipher whether Kv1.3 tyrosines may be involved in the EGF-dependent endocytosis, we mutated all of the internal tyrosines of the channel. The Kv1.3-Yless channel was fully functional and, similar to Kv1.3 wild-type, EGF inhibited K^+ currents, although to a lesser extent (Supplementary Fig. 3F,G). This diminished effect confirmed the role of Tyr phosphorylation on the Kv1.3 activity. Surprisingly, Kv1.3-Yless underwent EGF-dependent endocytosis, as observed by colocalization with intracellular EGF (Supplementary Fig. 3H–L). Therefore, our results confirm that the tyrosines within Kv1.3, which are involved in the EGF-dependent down regulation of the Kv1.3 activity, are not responsible for channel internalization. Accordingly, we also studied other Kv1.3 structural elements (Supplementary Fig. 4). Kv1.3 contains two proline-rich stretches (^{38}PLPPALP^{44} and ^{493}PQTP^{496}), which interact with SH3-containing signaling molecules in

the EGFR pathway. In addition, Kv1.3 possesses a PDZ domain at the distal C-terminal end that has been implicated in targeting the channel to membrane raft microdomains [37]. Both, the Kv1.3-Pless (no prolines, Supplementary Fig. 4F–J) and the Kv1.3T523X (no PDZ domain, Supplementary Fig. 4K–O) channels were endocytosed upon EGF incubation, similar to Kv1.3 wt (Supplementary Fig. 4A–E), demonstrating that those elements are not involved in EGF-mediated Kv1.3 endocytosis.

Activation of the EGF signaling cascade elicits a rapid phosphorylation of p42/44 MAPK (ERK1/2) [38]. ERK1/2 kinases participate in the suppression of ENaC activity [39]. To date, no ERK1/2 phosphorylation sites have been described in Kv1.3, although the channel contains a putative ERK phosphorylation consensus motif (^{493}PQTP^{496}). Therefore, we wondered whether a new, and not yet identified, ERK1/2 mechanism was responsible for the EGF-mediated Kv1.3 endocytosis (Fig. 5). We first analyzed ERK1/2 activation in the Kv1.3 HeLa cell line. The presence of EGF induced ERK1/2 phosphorylation (p42/44 MAPK) without varying their total amount (Fig. 5a). In this context, U0126, an inhibitor of ERK1/2, decreased the levels of P-ERK1/2 and counteracted the EGF-dependent decrease of biotinylated Kv1.3 at the cell surface. Concomitantly, U0126 blocked the EGF-dependent down regulation of Kv1.3 currents (Fig. 5b, c). These results indicate that ERK1/2 is indeed involved in the down-regulation of Kv1.3 by EGF. As mentioned above, the down-regulation of Kv1.3 by EGF has dual roles: (i) tyrosine kinase-dependent inhibition of K^+ currents and (ii) tyrosine kinase-independent mediated endocytosis. Therefore, we analyzed the role of ERK1/2 in EGF-dependent Kv1.3 endocytosis. EGF-dependent Kv1.3 endocytosis was efficiently neutralized by U0126 (Fig. 5d–m). Whether ERK1/2 kinases participated in the EGF-dependent Kv1.3 endocytosis was further analyzed in primary culture SVZ-derived cells (Fig. 6). ERK1/2 kinases were phosphorylated by EGF concomitantly to an increase of endocytosed Kv1.3 (Fig. 6a–f). In addition, EGF triggered the internalization of the EGFR which notably colocalized with endocytosed Kv1.3 (Fig. 6g–l). Finally, we mutated T495 within the putative ERK1/2 consensus motif of Kv1.3. The T495A mutation did not affect the Kv1.3 distribution in the absence of EGF (Fig. 7a). However, the EGF-mediated Kv1.3 (T495A) endocytosis was absent in the presence of EGF (Fig. 7b–e). Similar results were obtained with a glutamate mutation of the T495 (not shown). Concomitantly, Kv1.3 (T495A) currents were not down-regulated by EGF (Fig. 7f–g). Furthermore, unlike Kv1.3 wt, the T495A mutant underwent no Thr-phosphorylation upon EGF incubation (Fig. 7h). Our data demonstrated that ERK1/2 kinases specifically mediate the EGF-dependent Kv1.3 endocytosis through T495 phosphorylation, which is located at the C-terminal domain of the channel.

Discussion

Evidence indicates that the abundance of ion channels at the cell membrane is a crucial factor controlling their signal intensity. Thus, deciphering the mechanisms regulating the balance between forward traffic and internalization are essential. Ion channels, such as ENaC, Kv1.2, Kir1.1 and CFTR, undergo endocytosis via CCP through tyrosine kinase-dependent and -independent phosphorylation, and this mechanism is involved in controlling channel surface levels and activity [23, 25, 26, 40]. In this scenario, although Kv1.3 tyrosine kinase phosphorylation and its consequences have been extensively studied in lymphocytes

and neurons, no internalization evidence had been observed. Using an extensive repertoire of complementary techniques, we demonstrate here that Kv1.3 undergoes notable EGF-induced CME via a novel mechanism that involves p42/44 MAPK (ERK1/2) kinases. EGF and Kv1.3 inhibition act synergistically in the proliferative behavior of NSC from the SVZ. Kv1.3 activity is reduced by EGFR activation in an unconventional dual pathway, comprising both tyrosine phosphorylation-dependent inhibition of channel activity and threonine phosphorylation-dependent internalization of the channel. Together, these results suggest that Kv1.3 activity is quickly reduced by EGF with important consequences in neurogenesis.

The adult mammalian brain contains NSC that generate neurons and glia cells throughout the whole life of an organism [41]. NSC reside in at least two proliferative niches in the adult brain, the SVZ of the lateral ventricles and the subgranular zone of the hippocampus [41]. EGF is a potent mitogen that triggers the proliferation, survival, migration and differentiation of neurons and SVZ type-B astrocytes [4]. Cell proliferation in the SVZ supplies new neurons that eventually become incorporated into the existing functional brain networks [41]. The EGF-stimulated progenitors are highly migratory, which facilitates neural tissue repair [42]. On the other hand, Kv1.3 is implicated in cell growth and differentiation of a wide diversity of cells [11, 43]. Kv1.3 is selectively distributed in the OB, the cerebral cortex, the dentate gyrus of the hippocampus and in brain progenitor cells [44]. The involvement of Kv1.3 in controlling the proliferation of adult neural precursor cells (NPC) remains controversial. Although some authors could not confirm the pharmacological expression of Kv1.3 in adult NPC, others identified gene and protein expression in adult rat mesencephalic-derived neurospheres, NPCs and oligodendrocyte progenitor cells (OPCs) [43, 45–47]. We found Kv1.3 in both the SVZ in vivo and in NSCs derived from the SVZ. We also detect functional Kv1.3 channels in progenitor cells from neurospheres derived from the posterior SVZ (pSVZ). Selective blockage of Kv1.3 increased adult murine mes-encephalic NPC proliferation, using the model of long-term cultured neurospheres under non-differentiating conditions. Furthermore, granzyme B (GrB) released by T cells increased the expression of Kv1.3 within NPC, inhibiting proliferation and neuronal differentiation [48]. Our results showed a reinforcement of the EGF effect by blocking Kv1.3 on SVZ-derived explants. This suggests that EGFR activation and down-regulation of Kv1.3 acts synergistically to promote NSC proliferation and migration.

In agreement with the EGFR/Kv1.3 colocalization in the SVZ of the brain, receptor tyrosine kinases, such as EGFR and the insulin receptor, target Kv1.3 activity by tyrosine phosphorylation of the channel without endocytosis [27]. The balance between forward traffic and internalization fine tunes ion channel surface abundance and function [22]. The specific molecular mechanisms mediating K^+ channel endocytosis are poorly understood. In this vein, a dominant negative form of dynamin blocks Kv1.2 internalization, and Kir1.1 is also regulated by tyrosine kinases in a process involving dynamin and clathrin-dependent endocytosis [26, 40]. Furthermore, ENac is present in CCP and co-immunoprecipitates with clathrin adaptor proteins [23].

We observed a major colocalization between Kv1.3 and EGFR in internalized vesicles after EGF addition, and the depletion of dynamin II and CHC with specific siRNAs supported a

CCP-dependent mechanism of Kv1.3 internalization. As we demonstrated, Kv1.3 current reduction in the presence of EGF is also partially due to CCP-mediated channel endocytosis, but unlike Kv1.2 and Kir1.1, this mechanism was independent of tyrosine kinase phosphorylation of the channel [26, 40]. Thus, an Y132F mutation within the N-terminus of Kv1.2 confers resistance to phosphorylation-dependent suppression of Kv1.2 ionic currents and to channel endocytosis. Although Kv1.3 has several tyrosines, only Y479 has been described as being responsible for EGFR-mediated Kv1.3 current suppression, and non-specific channel internalization was postulated as a potential accompanying mechanism [8]. Phosphorylated tyrosines could be recognized by a variety of src homology 2 (SH2) domain-containing proteins. The adaptor protein nShc contains a SH2 domain and interacts with Kv1.3. However, our Kv1.3 (Y-less) mutant confirms and extents previous data indicating that SH2-interacting mechanisms are not involved in EGFR-dependent Kv1.3-mediated endocytosis. Several partners could link EGFR activation and downstream signaling cascades with channel endocytosis. Grb10 is a SH3 (Src homology 3) adaptor protein that co-immunoprecipitates with Kv1.3 in the OB and hippocampus [17]. SH3 domains mediate assembly of specific protein complexes by binding to proline-rich signatures in their targets. In this respect, Kv1.5 regulation by tyrosine kinases involves the SH3 domain-mediated physical interaction of src kinase with the channel protein [15]. Furthermore, PSD-95, an adaptor which contains PDZ and SH3 domains, interacts with Kv1.3 through a PDZ domain at the C-terminal end of the channel [37]. The PSD-95 SH3-guanylate kinase (GK) domain functionally modulates Kv1.3 and blocks the insulin-dependent channel phosphorylation [49]. However, our results indicate that these canonical Kv1.3 motifs, which interact with adaptor partners, were not involved in EGF-induced Kv1.3 endocytosis. Moreover, these experiments strongly reinforce that EGFR does not physically interact with Kv1.3. Alternatively, EGF controls sodium absorption, modulating ENaC surface expression via ERK1/2 activation in renal cells independent of tyrosine kinase activity [39]. Surprisingly, no ERK1/2 phosphorylation had been described for Kv1.3. Unlike other K^+ channels, Kv1.3 would be modulated by EGF similarly to ENaC, affecting neural stem cell fate. It is tempting to speculate that because Kv1.3 is the major K^+ channel entity in the sensory neuron physiology, EGF effectively regulates the channel in a dual unconventional pathway, which is comprised of both tyrosine phosphorylation-dependent inhibition of the activity, common to K^+ channels, and threonine phosphorylation-dependent internalization to fine tune cell responses.

In summary, we demonstrated that EGF triggers Kv1.3 current down-regulation by tyrosine phosphorylation and also a CME via a new, unconventional ERK1/2 kinase-dependent mechanism. Our results have important physiological significance. Kv1.3 is emerging as a promising target for developing new pharmacological agents against inflammation-associated neurodegenerative diseases, such as multiple sclerosis (MS) or brain infarction. Elevated levels of Kv1.3 may be associated with a negative prognosis in autoimmune neurodegenerative diseases [50, 51]. Moreover, EGFR signaling in vivo is involved in oligodendrocyte development and remyelination repair. Accordingly, EGF administration has been used therapeutically to counteract demyelination processes [52]. Our results show an additive effect of EGF in SVZ-derived progenitors when Kv1.3 is also pharmacologically inhibited. It is tempting to speculate a putative synergistic role of EGF-signaling and Kv1.3

function in controlling the multiple and complementary pathways during the progression of demyelinating disorders. As a consequence, modulation of these two elements may control the progression of neurodegenerative diseases. Kv1.3 inhibition with therapeutic compounds, such as analogs of a sea anemone toxin or psoralene derivatives, would decrease the cytotoxic effect of MS-infiltrates acting simultaneously on activated lymphocytes and proliferating OPCs [53, 54]. Thus, EGF supplementation might be a useful adjunctive for Kv1.3 inhibition in the treatment of MS and brain damage (e.g., after hypoxia). Simultaneous control of EGF activity and Kv1.3 function may provide a more effective way to control the growth, proliferation and differentiation of stem cells used for the treatment of neurodegenerative disorders or regeneration of the CNS.

Supplementary Material

Refer to Web version on PubMed Central for supplementary material.

Acknowledgments

Supported by the Ministerio de Economía y Competitividad (MINECO), Spain (BFU2014-54928-R and CSD2008-00005 to AF; SAF2013-42445-R to ES). MPV and KS hold fellowships from the MINECO. RMM and NC were supported by the Juan de la Cierva program (MINECO). AS was supported by NIH grants DA014204 and CA089151.

References

1. Lledo PM, Alonso M, Grubb MS. Adult neurogenesis and functional plasticity in neuronal circuits. Nat Rev Neurosci. 2006; 7:179–193. [PubMed: 16495940]
2. Menezes JR, Smith CM, Nelson KC, Luskin MB. The division of neuronal progenitor cells during migration in the neonatal mammalian forebrain. Mol Cell Neurosci. 1995; 6:496–508. [PubMed: 8742267]
3. Lichtenwalner RJ, Parent JM. Adult neurogenesis and the ischemic forebrain. J Cereb Blood Flow Metab. 2006; 26:1–20. [PubMed: 15959458]
4. Doetsch F, Petreanu L, Caille I, Garcia-Verdugo JM, Alvarez-Buylla A. EGF converts transit-amplifying neurogenic precursors in the adult brain into multipotent stem cells. Neuron. 2002; 36:1021–1034. [PubMed: 12495619]
5. Wong RW, Guillaud L. The role of epidermal growth factor and its receptors in mammalian CNS. Cytokine Growth Factor Rev. 2004; 15:147–156. [PubMed: 15110798]
6. Sashihara S, Tsuji S, Matsui T. Oncogenes and signal transduction pathways involved in the regulation of Na+ channel expression. Crit Rev Oncog. 1998; 9:19–34. [PubMed: 9754445]
7. Hille, B. Ion channels of excitable membranes. 3. Sinauer; Sunderland: 2001.
8. Fadool DA, Levitan IB. Modulation of olfactory bulb neuron potassium current by tyrosine phosphorylation. J Neurosci. 1998; 18:6126–6137. [PubMed: 9698307]
9. Doczi MA, Morielli AD, Damon DH. Kv1.3 channels in postganglionic sympathetic neurons: expression, function, and modulation. Am J Physiol Regul Integr Comp Physiol. 2008; 295:R733–R740. [PubMed: 18614767]
10. Fadool DA, Tucker K, Perkins R, Fasciani G, Thompson RN, Parsons AD, Overton JM, Koni PA, Flavell RA, Kaczmarek LK. Kv1.3 channel gene-targeted deletion produces “Super-Smeller Mice” with altered glomeruli, interacting scaffolding proteins, and biophysics. Neuron. 2004; 41:389–404. [PubMed: 14766178]
11. Vicente R, Escalada A, Coma M, Fuster G, Sanchez-Tillo E, Lopez-Iglesias C, Soler C, Solsona C, Celada A, Felipe A. Differential voltage-dependent K+ channel responses during proliferation and activation in macrophages. J Biol Chem. 2003; 278:46307–46320. [PubMed: 12923194]

12. Villalonga N, David M, Bielanska J, Gonzalez T, Parra D, Soler C, Comes N, Valenzuela C, Felipe A. Immunomodulatory effects of diclofenac in leukocytes through the targeting of Kv1.3 voltage-dependent potassium channels. Biochem Pharmacol. 2010; 80:858–866. [PubMed: 20488163]
13. Bowlby MR, Fadool DA, Holmes TC, Levitan IB. Modulation of the Kv1.3 potassium channel by receptor tyrosine kinases. J Gen Physiol. 1997; 110:601–610. [PubMed: 9348331]
14. Holmes TC, Fadool DA, Levitan IB. Tyrosine phosphorylation of the Kv1.3 potassium channel. J Neurosci. 1996; 16:1581–1590. [PubMed: 8774427]
15. Holmes TC, Fadool DA, Ren R, Levitan IB. Association of Src tyrosine kinase with a human potassium channel mediated by SH3 domain. Science. 1996; 274:2089–2091. [PubMed: 8953041]
16. Fadool DA, Tucker K, Phillips JJ, Simmen JA. Brain insulin receptor causes activity-dependent current suppression in the olfactory bulb through multiple phosphorylation of Kv1.3. J Neurophysiol. 2000; 83:2332–2348. [PubMed: 10758137]
17. Cook KK, Fadool DA. Two adaptor proteins differentially modulate the phosphorylation and biophysics of Kv1.3 ion channel by SRC kinase. J Biol Chem. 2002; 277:13268–13280. [PubMed: 11812778]
18. Colley B, Tucker K, Fadool DA. Comparison of modulation of Kv1.3 channel by two receptor tyrosine kinases in olfactory bulb neurons of rodents. Receptors Channels. 2004; 10:25–36. [PubMed: 14769549]
19. Vicente R, Villalonga N, Calvo M, Escalada A, Solsona C, Soler C, Tamkun MM, Felipe A. Kv1.5 association modifies Kv1.3 traffic and membrane localization. J Biol Chem. 2008; 283:8756–8764. [PubMed: 18218624]
20. Villalonga N, Escalada A, Vicente R, Sanchez-Tillo E, Celada A, Solsona C, Felipe A. Kv1.3/Kv1.5 heteromeric channels compromise pharmacological responses in macrophages. Biochem Biophys Res Commun. 2007; 352:913–918. [PubMed: 17157812]
21. Sole L, Roura-Ferrer M, Perez-Verdaguer M, Oliveras A, Calvo M, Fernandez-Fernandez JM, Felipe A. KCNE4 suppresses Kv1.3 currents by modulating trafficking, surface expression and channel gating. J Cell Sci. 2009; 122:3738–3748. [PubMed: 19773357]
22. Martinez-Marmol R, Perez-Verdaguer M, Roig SR, Vallejo-Gracia A, Gotsi P, Serrano-Albarras A, Bahamonde MI, Ferrer-Montiel A, Fernandez-Ballester G, Comes N, Felipe A. A non-canonical di-acidic signal at the C-terminus of Kv1.3 determines anterograde trafficking and surface expression. J Cell Sci. 2013; 126:5681–5691. [PubMed: 24144698]
23. Shimkets RA, Lifton RP, Canessa CM. The activity of the epithelial sodium channel is regulated by clathrin-mediated endocytosis. J Biol Chem. 1997; 272:25537–25541. [PubMed: 9325269]
24. Mankouri J, Taneja TK, Smith AJ, Ponnambalam S, Sivaprasadarao A. Kir6.2 mutations causing neonatal diabetes prevent endocytosis of ATP-sensitive potassium channels. EMBO J. 2006; 25:4142–4151. [PubMed: 16902404]
25. Lukacs GL, Segal G, Kartner N, Grinstein S, Zhang F. Constitutive internalization of cystic fibrosis transmembrane conductance regulator occurs via clathrin-dependent endocytosis and is regulated by protein phosphorylation. Biochem J. 1997; 328(Pt 2):353–361. [PubMed: 9371688]
26. Nesti E, Everill B, Morielli AD. Endocytosis as a mechanism for tyrosine kinase-dependent suppression of a voltage-gated potassium channel. Mol Biol Cell. 2004; 15:4073–4088. [PubMed: 15215309]
27. Fadool DA, Holmes TC, Berman K, Dagan D, Levitan IB. Tyrosine phosphorylation modulates current amplitude and kinetics of a neuronal voltage-gated potassium channel. J Neurophysiol. 1997; 78:1563–1573. [PubMed: 9310443]
28. Gonzalez-Perez O, Quinones-Hinojosa A. Dose-dependent effect of EGF on migration and differentiation of adult subventricular zone astrocytes. Glia. 2010; 58:975–983. [PubMed: 20187143]
29. Chazal G, Durbec P, Jankovski A, Rougon G, Cremer H. Consequences of neural cell adhesion molecule deficiency on cell migration in the rostral migratory stream of the mouse. J Neurosci. 2000; 20:1446–1457. [PubMed: 10662835]
30. Fontana X, Nacher J, Soriano E, del Rio JA. Cell proliferation in the adult hippocampal formation of rodents and its modulation by entorhinal and fimbria-fornix afferents. Cereb Cortex. 2006; 16:301–312. [PubMed: 15958781]

31. Carter RE, Sorkin A. Endocytosis of functional epidermal growth factor receptor-green fluorescent protein chimera. J Biol Chem. 1998; 273:35000–35007. [PubMed: 9857032]
32. Fortian A, Sorkin A. Live-cell fluorescence imaging reveals high stoichiometry of Grb2 binding to the EGF receptor sustained during endocytosis. J Cell Sci. 2014; 127:432–444. [PubMed: 24259669]
33. Llado A, Tebar F, Calvo M, Moreto J, Sorkin A, Enrich C. Protein kinaseCdelta-calmodulin crosstalk regulates epidermal growth factor receptor exit from early endosomes. Mol Biol Cell. 2004; 15:4877–4891. [PubMed: 15342779]
34. Sorkina T, Miranda M, Dionne KR, Hoover BR, Zahniser NR, Sorkin A. RNA interference screen reveals an essential role of Nedd4-2 in dopamine transporter ubiquitination and endocytosis. J Neurosci. 2006; 26:8195–8205. [PubMed: 16885233]
35. Huang F, Khvorova A, Marshall W, Sorkin A. Analysis of clathrin-mediated endocytosis of epidermal growth factor receptor by RNA interference. J Biol Chem. 2004; 279:16657–16661. [PubMed: 14985334]
36. Sorkina T, Hoover BR, Zahniser NR, Sorkin A. Constitutive and protein kinase C-induced internalization of the dopamine transporter is mediated by a clathrin-dependent mechanism. Traffic. 2005; 6:157–170. [PubMed: 15634215]
37. Szilagyi O, Boratko A, Panyi G, Hajdu P. The role of PSD-95 in the rearrangement of Kv1.3 channels to the immunological synapse. Pflugers Arch. 2013; 465:1341–1353. [PubMed: 23553419]
38. Galperin E, Abdelmoti L, Sorkin A. Shoc2 is targeted to late endosomes and required for Erk1/2 activation in EGF-stimulated cells. PLoS ONE. 2012; 7:e36469. [PubMed: 22606262]
39. Booth RE, Stockand JD. Targeted degradation of ENaC in response to PKC activation of the ERK1/2 cascade. Am J Physiol Renal Physiol. 2003; 284:F938–F947. [PubMed: 12540365]
40. Zeng WZ, Babich V, Ortega B, Quigley R, White SJ, Welling PA, Huang CL. Evidence for endocytosis of ROMK potassium channel via clathrin-coated vesicles. Am J Physiol Renal Physiol. 2002; 283:F630–F639. [PubMed: 12217853]
41. Ming GL, Song H. Adult neurogenesis in the mammalian brain: significant answers and significant questions. Neuron. 2011; 70:687–702. [PubMed: 21609825]
42. Gonzalez-Perez O, Romero-Rodriguez R, Soriano-Navarro M, Garcia-Verdugo JM, Alvarez-Buylla A. Epidermal growth factor induces the progeny of subventricular zone type B cells to migrate and differentiate into oligodendrocytes. Stem Cells. 2009; 27:2032–2043. [PubMed: 19544429]
43. Chittajallu R, Chen Y, Wang H, Yuan X, Ghiani CA, Heckman T, McBain CJ, Gallo V. Regulation of Kv1 subunit expression in oligodendrocyte progenitor cells and their role in G1/S phase progression of the cell cycle. Proc Natl Acad Sci U S A. 2002; 99:2350–2355. [PubMed: 11854528]
44. Kues WA, Wunder F. Heterogeneous expression patterns of mammalian potassium channel genes in developing and adult rat brain. Eur J Neurosci. 1992; 4:1296–1308. [PubMed: 12106393]
45. Yasuda T, Bartlett PF, Adams DJ. K(ir) and K(v) channels regulate electrical properties and proliferation of adult neural precursor cells. Mol Cell Neurosci. 2008; 37:284–297. [PubMed: 18023363]
46. Liebau S, Propper C, Bockers T, Lehmann-Horn F, Storch A, Grissmer S, Wittekindt OH. Selective blockage of Kv1.3 and Kv3.1 channels increases neural progenitor cell proliferation. J Neurochem. 2006; 99:426–437. [PubMed: 17029597]
47. Tegla CA, Cudrici C, Rozycka M, Soloviova K, Ito T, Singh AK, Khan A, Azimzadeh P, Andrian-Albescu M, Niculescu F, Rus V, Judge SI, Rus H. C5b-9-activated, K(v)1.3 channels mediate oligodendrocyte cell cycle activation and dedifferentiation. Exp Mol Pathol. 2011; 91:335–345. [PubMed: 21540025]
48. Wang T, Lee MH, Johnson T, Allie R, Hu L, Calabresi PA, Nath A. Activated T-cells inhibit neurogenesis by releasing granzyme B: rescue by Kv1.3 blockers. J Neurosci. 2010; 30:5020–5027. [PubMed: 20371822]
49. Marks DR, Fadool DA. Post-synaptic density perturbs insulin-induced Kv1.3 channel modulation via a clustering mechanism involving the SH3 domain. J Neurochem. 2007; 103:1608–1627. [PubMed: 17854350]

50. Rus H, Pardo CA, Hu L, Darrah E, Cudrici C, Niculescu T, Niculescu F, Mullen KM, Allie R, Guo L, Wulff H, Beeton C, Judge SI, Kerr DA, Knaus HG, Chandy KG, Calabresi PA. The voltage-gated potassium channel Kv1.3 is highly expressed on inflammatory infiltrates in multiple sclerosis brain. Proc Natl Acad Sci U S A. 2005; 102:11094–11099. [PubMed: 16043714]

51. Varga Z, Csepany T, Papp F, Fabian A, Gogolak P, Toth A, Panyi G. Potassium channel expression in human CD4+ regulatory and naive T cells from healthy subjects and multiple sclerosis patients. Immunol Lett. 2009; 124:95–101. [PubMed: 19409928]

52. Scalabrino G, Tredici G, Buccellato FR, Manfridi A. Further evidence for the involvement of epidermal growth factor in the signaling pathway of vitamin B12 (cobalamin) in the rat central nervous system. J Neuropathol Exp Neurol. 2000; 59:808–814. [PubMed: 11005261]

53. Vennekamp J, Wulff H, Beeton C, Calabresi PA, Grissmer S, Hansel W, Chandy KG. Kv1.3-blocking 5-phenylalkoxypsoralens: a new class of immunomodulators. Mol Pharmacol. 2004; 65:1364–1374. [PubMed: 15155830]

54. Norton RS, Pennington MW, Wulff H. Potassium channel blockade by the sea anemone toxin ShK for the treatment of multiple sclerosis and other autoimmune diseases. Curr Med Chem. 2004; 11:3041–3052. [PubMed: 15578998]

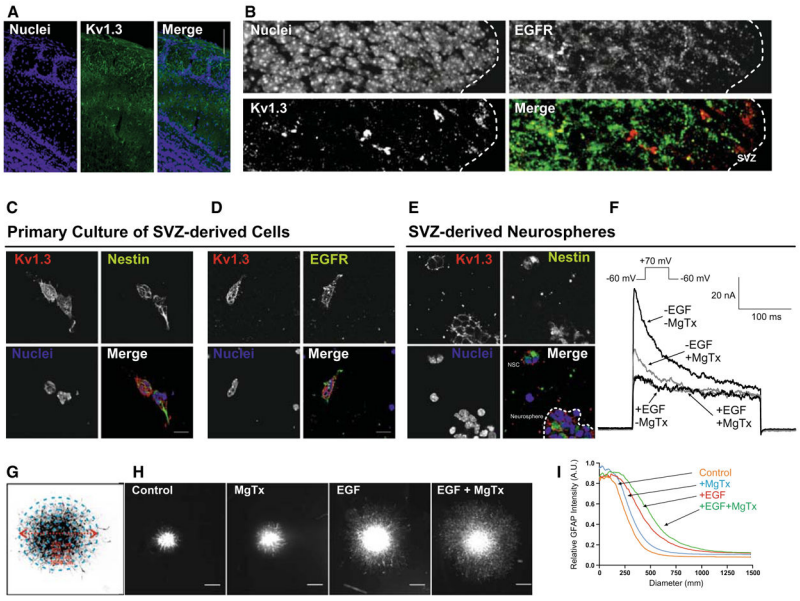

Fig. 1.

Kv1.3 and EGFR colocalized in the brain and neuronal precursor cells. **a** Kv1.3 is present in the OB. OB slices were obtained and stained for Kv1.3 (*green*) and DAPI (*blue*). *Bar* represents 20 μm. **b** Kv1.3 colocalized with EGFR in the SVZ of the forebrain. SVZ explants were analyzed for Kv1.3 and EGFR. The *merge panel* indicates colocalization (*yellow*) within the SVZ. **c**, **d** Kv1.3 and EGFR colocalized in primary cultures of SVZ-derived cells. **c** Kv1.3 colocalized with Nestin, a marker of neuronal precursors. **d** Kv1.3 colocalized with EGFR in Nestin-positive cells. The *merge panels* indicate colocalization of these proteins in the same cell. **e** Expression of Kv1.3 in SVZ-derived neurospheres. Neurospheres were obtained from SVZ-derived cells and cultured as described in the "Materials and Methods". Nestin was used as a marker for NSCs. The *merge panel* highlights the expression of Kv1.3 in Nestin-positive neurospheres. **f** Voltage-dependent K^+ currents were evoked in neurospheres, incubated with or without EGF, as indicated by pulse protocols. Currents were inhibited by 100 nM Margatoxin only in the absence of EGF. **g–i** Effects of EGF and MgTx on the migration and differentiation of SVZ astrocytes. **g** GFAP intensity and distance from the core of the spot was used as a marker of differentiation and migration. **h** $GFAP^+$ cells (n = 10–15) were incubated in the presence and the absence of EGF and MgTx and images were captured for quantification. *Bars* represent 500 μm. **i** Quantification of the relative GFAP intensity from the core of the spot. Note that the incubation of EGF plus MgTx (*green*) was additive over EGF (*red*) or MgTx (*blue*) alone

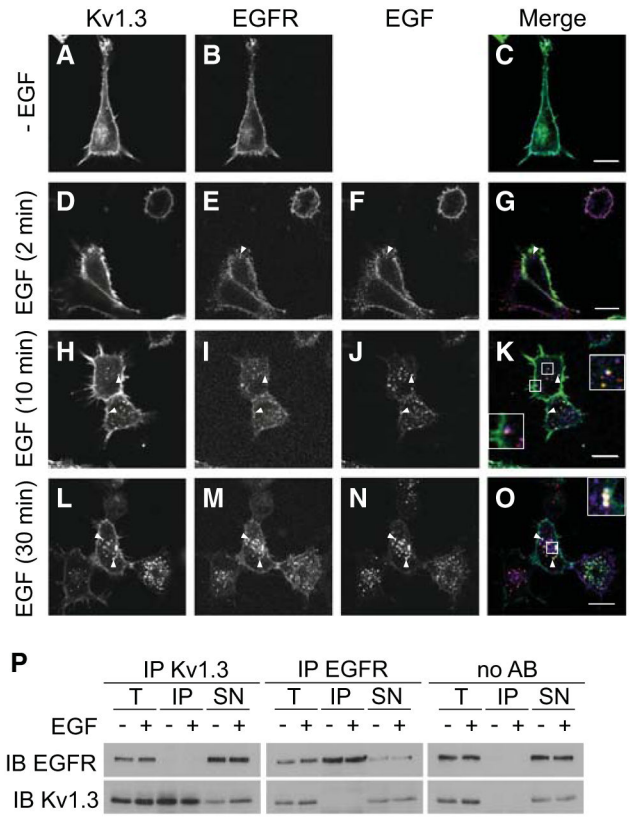

Fig. 2.

EGF steadily increased Kv1.3 colocalization, but did not promote association with endocytosed EGFR. **a**–**o** Representative confocal images of HEK293 cells that were transiently co-transfected with Kv1.3-YFP (**a**, **d**, **h**, **l**, and *green in merge panels*) and EGFR-CFP (**b**, **e**, **i**, **m**, and *blue in merge panels*). Cells were incubated with 10 ng/ml EGF-rhodamine (**f**, **j**, **n**, and *red in merge panels*) for 2, 10 and 30 min at 37 °C. EGF-dependent EGFR endocytic vesicles (*pink*) were seen after 2 min (*arrowheads* in **e**–**g**). However, triple EGF-dependent EGFR and Kv1.3-containing vesicles (*white*) were observed after longer times of EGF incubation (*arrowheads* in **k** and **o**). *Insets* show magnification areas. *Bars* represent 10 μm. **p** Kv1.3 did not co-immunoprecipitate with EGFR. Cells were co-transfected with HA-Kv1.3 and EGFR-CFP and incubated in the presence (+) or in the absence (−) of 10 ng/ml EGF for 15 min. Lysates were immunoprecipitated (IP) with anti-HA (Kv1.3) and anti-GFP (EGFR) antibodies. No AB, absence of antibody. Filters were immunoblotted (IB) with anti-HA (Kv1.3) and anti-GFP (EGFR) antibodies. No co-IP was observed between the channel and the receptor. *T* total lysate, *IP* immunoprecipitate, *SN* supernatant

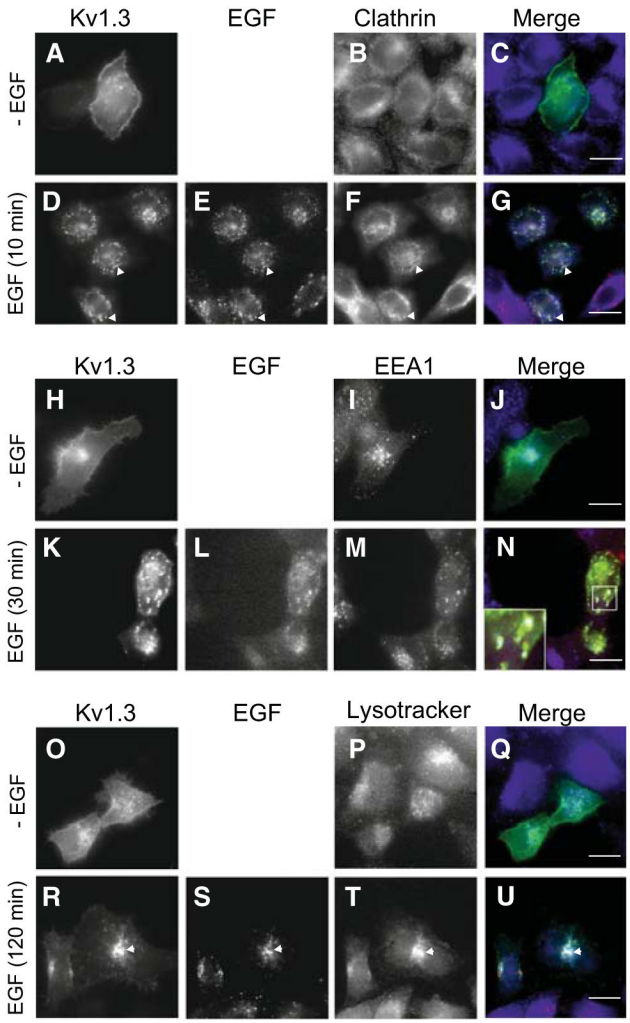

Fig. 3.

Deciphering the steadily EGF-dependent Kv1.3 internalization pathway with endocytic markers in HeLa cells. Representative confocal images of HeLa cells that stably express Kv1.3-YFP. Cells were incubated in the absence (−EGF) or presence (+EGF) of EGF-rhodamine (4 ng/ml) at 37 °C during different times. (**a**–**g**) Cells were incubated for 10 min and stained with antibodies against CHC. (**h**–**n**) Cells were incubated for 30 min and stained with an anti-EEA1 antibody. (**o**–**u**) Cells were incubated with EGF-rhodamine for 120 min and with 50 nM LysoTracker for 30 min. Upon EGF incubation, triple colocalization was observed in structures containing Kv1.3, EGF and clathrin (**d**–**g**, *arrowheads*); Kv1.3, EGF and EEA1 (**n**, *inset*); and Kv1.3, EGF and LysoTracker (**r**–**u**, *arrowhead*). Color code in *merge panels*: Kv1.3 (*green*), EGF (*red*) and markers (*blue*). *Bars* represent 10 μm

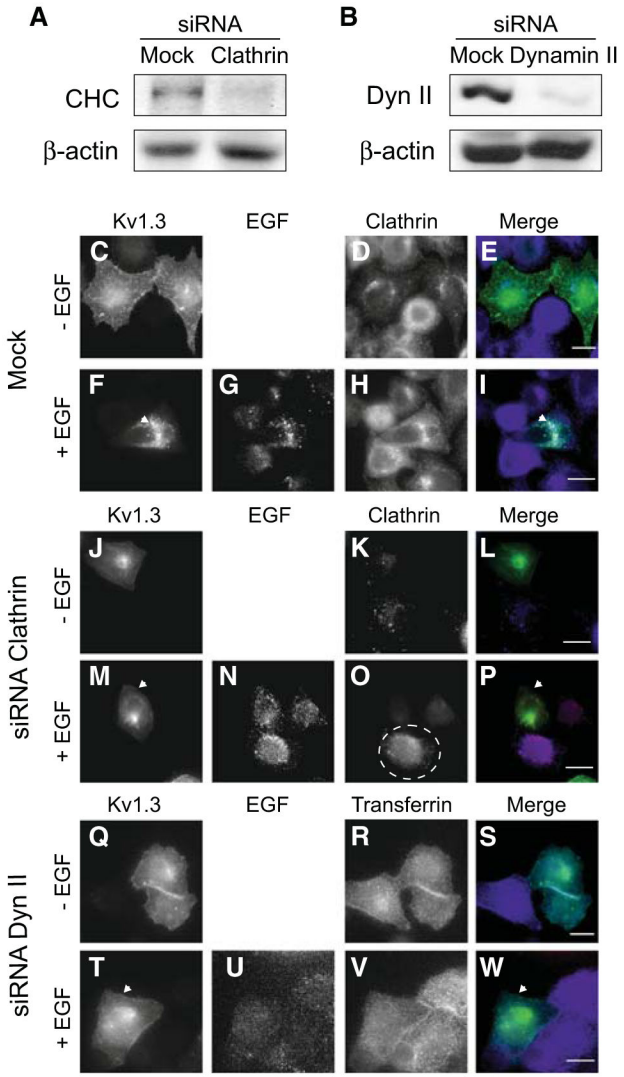

Fig. 4.

EGF-dependent Kv1.3 internalization is governed by clathrin-mediated endocytosis. Confocal images and western blot analysis of HeLa cells stably expressing Kv1.3-YFP. Cells were transfected without (Mock) or with siRNAs against Clathrin Heavy Chain (CHC) and Dynamin II (Dyn II). Cell lysates were blotted with antibodies against Clathrin, Dyn II, and β-actin. Western blots demonstrated the depletion of CHC (**a**) and Dyn II (**b**). (**c**–**w**) Cells mock transfected (**c**–**i**) or transfected with siRNAs to CHC (**j**–**p**) or Dyn II (**q**–**w**) were incubated with (+EGF) or without (−EGF) 4 ng/ml EGF-rhodamine for 30 min at 37 °C. **c**–**p** Cells were stained with anti-Clathrin antibodies. **q**–**w** Cells were also incubated in the presence of Transferrin-Texas Red (5 μg/ml). As observed in **a**, low numbers of clathrin-positive cells were found and *circled* in **o**. Color code in *merge panels*: Kv1.3 (*green*), EGF (*red*) and clathrin/transferrin (*blue*). *Arrowheads* highlight Kv1.3 either intracellular (**f**–**i**) or at the membrane (**m**–**p** and **t**–**w**). *Bars* represent 10 μm

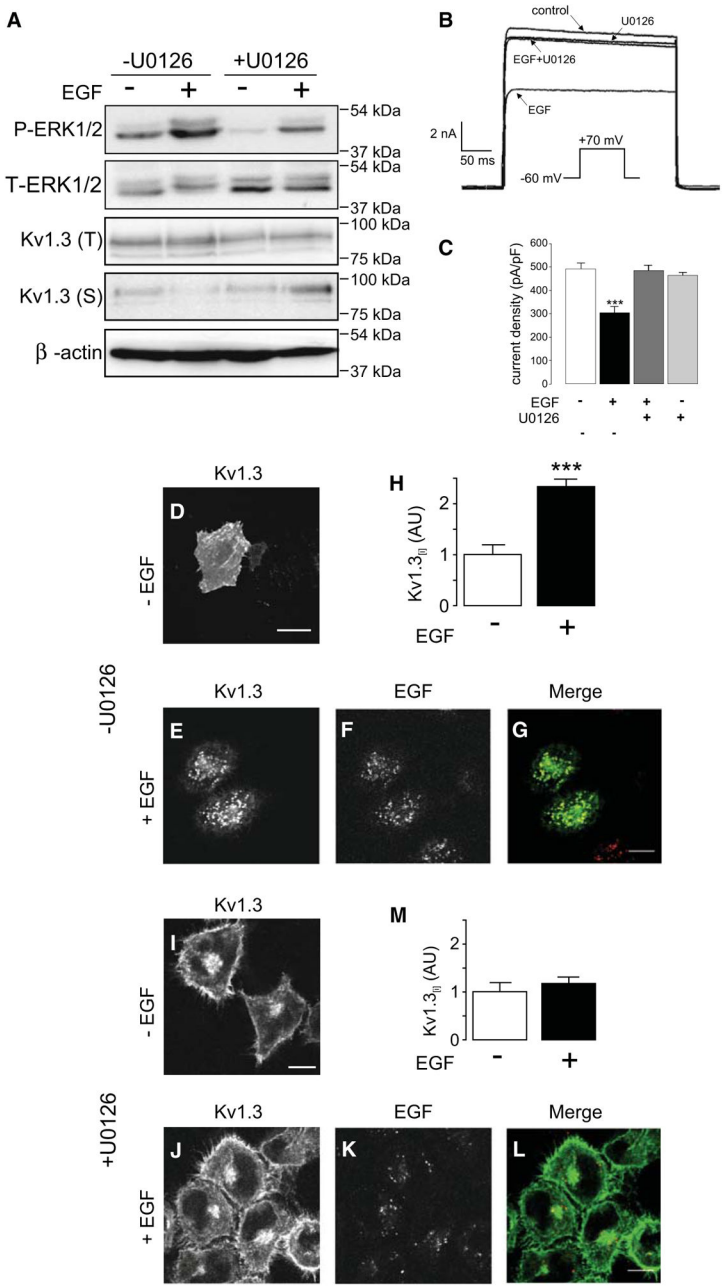

Fig. 5.

Effect of ERK1/2 activity on EGF-dependent Kv1.3 endocytosis. HeLa cells stably expressing Kv1.3-YFP were treated for 15 min prior to and during EGF stimulation with (+) or without (−) 10 μM U0126. Cells were incubated with (+EGF) or without (−EGF) 4 ng/ml EGF-rhodamine for 30 min at 37 °C. **a** Western blot analysis for active/phosphorylated ERK (p-ERK1/2) and biotinylated Kv1.3 at the cell surface in the presence (+) or the absence (−) of U0126 with (+) or without (−) EGF. Filters were further reprobed for total ERK (T-ERK1/2) and β-actin as loading controls. Note that upon EGF incubation, the induction of P-ERK1/2 was notably affected by presence of U0126. Furthermore, while the total expression

of Kv1.3 (T) remained similar, the amount of Kv1.3 at the surface (S) was reduced by EGF in the absence of U0126. **b** Voltage-dependent K^+ currents were evoked by a 250 ms depolarizing pulse from −60 to +70 mV. U0126 halted the EGF-dependent inhibition of K^+ currents. **c** Current density in pA/pF. ***P <0.001 vs—EGF (*white column*) (Student's t test). The results are the mean ± SEM of 8–10 cells. (**d**–**m**) Representative images of Kv1.3 HeLa cells in the presence (+) or the absence (−) of EGF with (+) or without (−) U0126. **d**–**g** EGF-dependent Kv1.3 endocytosis in the absence of U0126. **i**–**m** EGF-dependent Kv1.3 endocytosis in the presence of U0126. **g**, **l** Kv1.3 (*green*) and EGF (*red*) in *merge panels*. (**h**, **m**) Relative quantification of intracellular Kv1.3 ($Kv1.3_{[i]}$) in the absence (*white column*) or the presence (*black column*) of EGF with (**m**) and without (**h**) U0126. ***P <0.001 vs absence of EGF (Student's t test). The results are the mean ± SEM of 15–20 cells. Note that U0126 impaired the EGF-dependent Kv1.3 endocytosis. *Bars* represent 10 μm

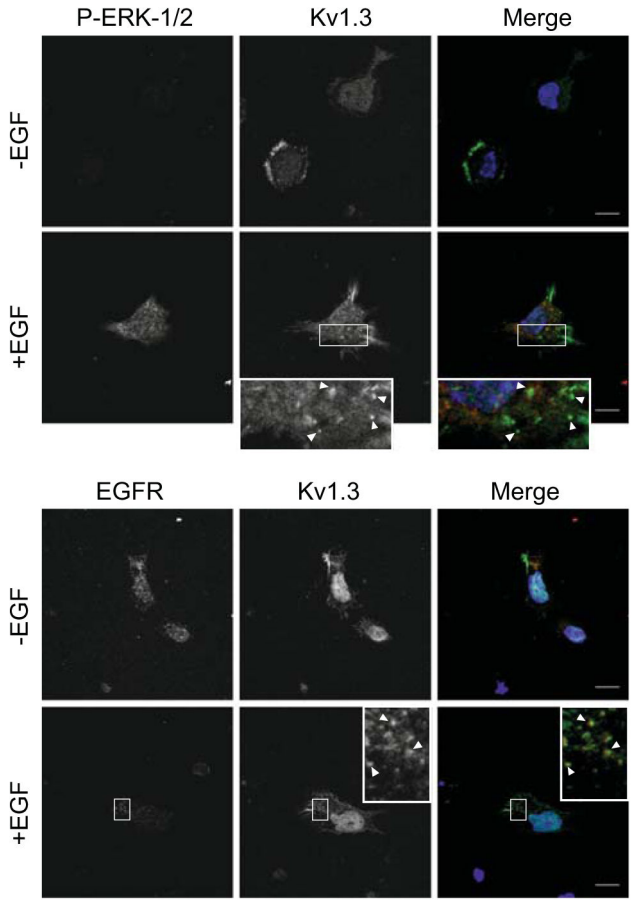

Fig. 6.

EGF-dependent ERK1/2 phosphorylation, EGFR internalization and Kv1.3 endocytosis in primary culture SVZ-derived cells. Cells were incubated with (+EGF) or without (−EGF) 10 ng/ml EGF for 15 min at 37 °C. **a**–**f** Representative images of P-ERK1/2 and Kv1.3. In the presence of EGF, activated form of ERK1/2 (P-ERK1/2) was homogeneously distributed throughout the cell whereas Kv1.3 concentrated in intracellular vesicles (see *inset* for details). **g**–**l** EGFR and Kv1.3 colocalized in intracellular vesicles in the presence of EGF (see *inset* for magnification). Color in *merge panels*: Kv1.3 in *green* (**c**, **f**, **i**, **l**), P-ERK1/2 in *red* (**c**, **f**) and EGF in *red* (**i**, **l**). *Arrow heads* highlight Kv1.3 enriched vesicles. *Bars* represent 10 μm

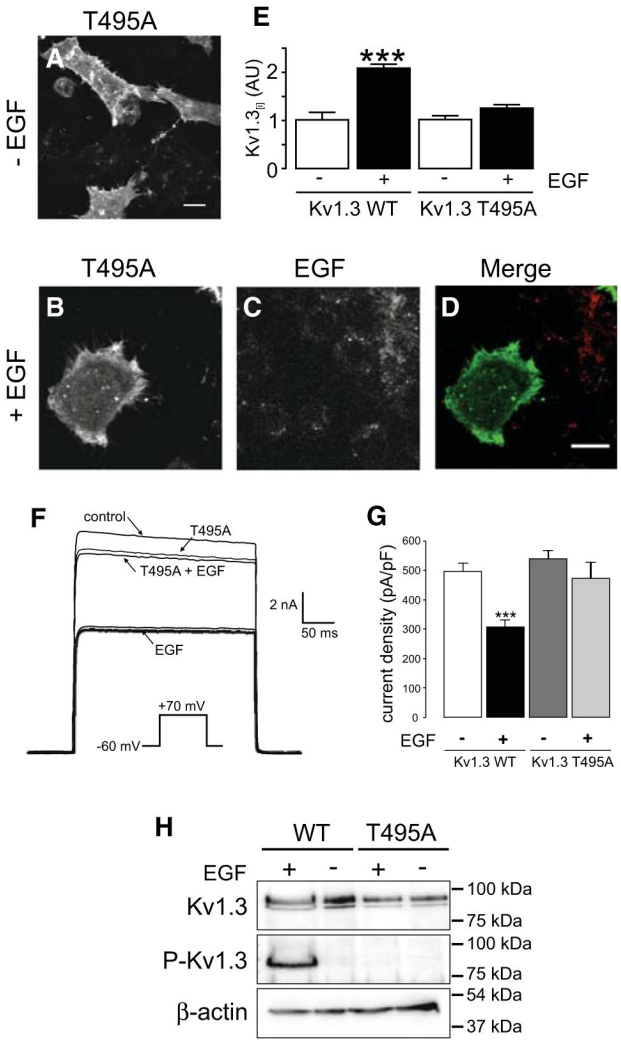

Fig. 7.

The Kv1.3 (T495A) mutant did not undergo EGF-dependent endocytosis. HeLa cells were transiently transfected with the Kv1.3-YFP (T495A) mutant channel. Cells were incubated with (+EGF) or without (−EGF) 4 ng/ml EGF-rhodamine for 30 min at 37 °C. **a**–**d** Representative images of Kv1.3 (T495A) in the presence (+) or the absence (−) of EGF. **a** Kv1.3 (T495A) in the absence of EGF. **b**–**d** Kv1.3 (T495A) in the presence of EGF. **d** Kv1.3 (*green*) and EGF (*red*) in *merge panel. Bars* represent 10 μm. **e** Relative quantification in arbitrary units (AU) of intracellular (Kv1.3$_{[i]}$) Kv1.3 wt and Kv1.3 (T495A) in the absence (*white column*) or the presence (*black column*) of EGF. ***P <0.001 vs Kv1.3 wt in the absence of EGF (Student's t-test). The results are the mean ± SEM of 15–25 cells. Note that Kv1.3 (T495A) did not undergo EGF-dependent Kv1.3 endocytosis. **f** Voltage-dependent K^+ currents were evoked by a 250 ms depolarizing pulse from −60 to +70 mV. **g** Current density in pA/pF. ***P <0.001 vs Kv1.3 wt in the absence of EGF (*white column*) (Student's t test). The results are the mean ± SEM of 8–10 cells. **h** Western blot analysis for total Kv1.3 and Thr-phosphorylated-Kv1.3 (P-Kv1.3) in the presence (+) or the absence (−) of EGF. Filters

were further reprobed for β-actin as loading control. Note that Kv1.3 (T495A) underwent no phosphorylation in Thr (P-Kv1.3) in the presence of EGF